The new Material Science Powder Diffraction beamline at ALBA Synchrotron

F. Fauth , I. Peral, C. Popescu, M. Knapp*
CELLS-ALBA, BP1413, 08290 Cerdanyola del Vallès, Barcelona, Spain
*(*Present affiliation) Karlsruhe Institute of Technology, 76344 Eggenstein-Leopoldshafen, Germany*
E-mail: ffauth@cells.es

The current report describes the installation and the preliminary commissioning of the Material Science Powder Diffraction (MSPD) beamline at the Spanish synchrotron ALBA-CELLS. The beamline is fully dedicated to powder diffraction techniques and consists of two experimental stations positioned in series: a High Pressure/Microdiffraction station and a High Resolution/High Throughput powder diffraction station.

Key words: Material Science Powder Diffraction (MSPD), beamline, Spanish synchrotron ALBA-CELLS

Introduction

The ALBA-CELLS synchrotron located in the Barcelona area is currently the most recent synchrotron source in Europe. Machine and beamline commissioning started at the end of 2010 and in mid 2011, respectively. The first official users started in May 2012. The facility operates seven beamlines from soft X-ray energies (Resonant Absorption Scattering, Photoemission Spectroscopy and Microscopy, X-Ray Microscopy) to hard X-Ray energies (Non Crystalline Diffraction, Absorption and Emission Spectroscopy, Macromolecular Crystallography, Powder Diffraction). The machine consists of a 268 m circumference storage ring with electrons accelerated to 3 GeV and with small emittance (4.8 nm rad). All but one beamline have insertion devices as their synchrotron radiation source. The electron current in the ring is foreseen to reach 400 mA in top up injection mode but will be 250 mA at an initial stage.

Beamline source and optics

The X-ray flux intensity for the MSPD beamline was expected to be continuous over an 8 to 50 keV energy spectrum. Moreover, the total and local (at monochromator) power load could not exceed 20kW and 900W, respectively. Hence the insertion device (ID) choice was for a

 0885-7156/2013/28(S2)/S2/1/$18.00

superconducting wiggler with 60.5 periods of 31 mm and a peak magnetic field of 2.1 T. Under these conditions, the deflection parameter and critical energy are K=6.08 and E_c=12.5 keV, respectively. At the typical energy of 30 keV, effective X-ray source size, divergence and flux are 620 x 85 μm^2, 1 x 0.16 $mrad^2$ and 1×10^{14} ph/s/0.1%bw within a 300 x 125 μrad^2 aperture, respectively. The latter aperture corresponds to the maximum fixed acceptance of the MSPD front end. Within the front end, a set of water cooled slits (supplier FMB Berlin) further allows tuning of both the horizontal and vertical aperture. The first optical elements after the front end are power reducing devices: a permanent 320 μm thick CVD pre-filter assembly, a permanent 150 μm thick CVD vacuum window and a variable filter assembly allowing 27 possible configurations of different filter types and/or thicknesses.

At 21 m downstream from the source is the collimating mirror whose purpose is to reduce the heat load downstream, reduce the vertical divergence and eliminate high energy harmonics. The mirror, supplied by CINEL, is a 1.2 m long silicon block, water cooled and with liquid "Galinstan" (eutectic alloy of Ga, In and Sn) ensuring thermal contact between the coolant and the mirror. A single motor actuation mechanism allows cylindrical curving of the mirror down to a 5 km radius. Since the mirror is fixed at a 2 mrad incident angle relative to the incoming beam, the vertical collimation and focalization at the Powder Station (35 m from the source) are reached with a 21 km and 8.4 km bending radius, respectively. The mirror has three material surfaces since, in addition to the uncoated Si substrate, there are two 19 mm wide stripes (~600 Å coating thickness) consisting of Rh and Pt. As can be seen in Fig 1a, each of the three stripes offers a characteristic reflectivity curve with energy cut off at approximately 15keV, 33keV and 41 keV for Si, Rh and Pt, respectively. This energy cut off distribution is used to select the optimum surface layer in order to eliminate the 3rd (or higher) harmonics of the energy spectrum that can propagate downstream of the monochromator. In order to operate in the 40-50 keV range, the mirror is moved out of the white beam. In that case, the heat load on the monochromator is lowered by reducing the beam size, either using the slit system at the front end and/or using an equivalent slit system positioned between the mirror and the monochromator. Note that having the option to operate either with or without the mirror means that all components downstream of the mirror have to be vertically adjustable (up to 56 mm offset at the PD station).

https://doi.org/10.1017/S0885715613000900 Published online by Cambridge University Press

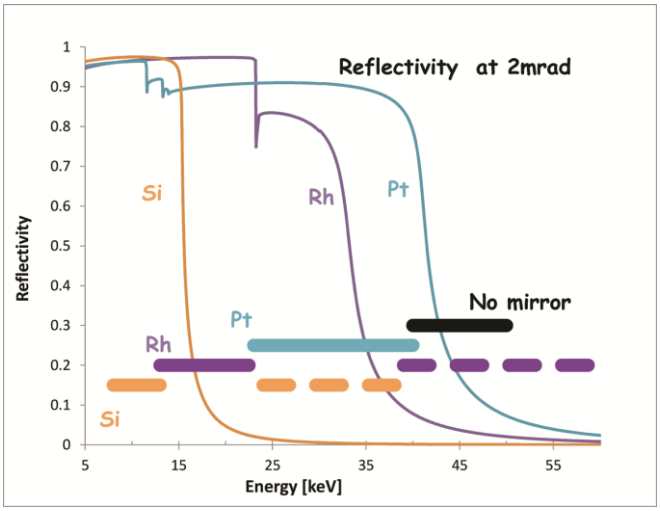

(a)

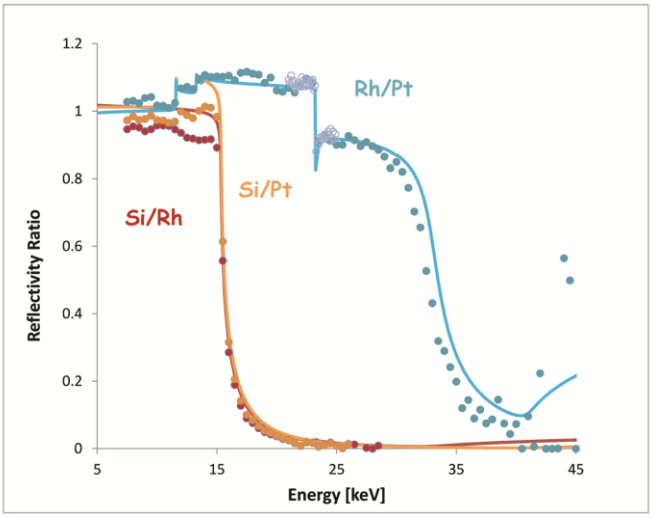

(b)

Figure 1: a) Calculated reflectivity of mirror coatings at 2 mrad incidence angle. The plain wide lines show the operating energy ranges of each coating, the dotted wide line the energy range which is suppressed by the mirror. b) Measured reflectivity ratio of rocking curves measured at selected stripes. Lines are the corresponding calculated ratio.

The fixed exit (20 mm offset) double crystal monochromator (DCM) is located 25 m downstream the source and was supplied by Bruker. Based on the double Bragg reflection of silicon (111) planes, it allows selection of X-ray energies down to $\Delta E/E \sim 10^{-4}$ resolution. In order to reduce the heat load impact on energy resolution, both crystals are directly cryogenically cooled. An additional water circulation allows thermalization of the crystal mounting mechanics, hence reducing long time mechanical drift due to white beam intensity variation (e.g. after a refill or machine shutdown). The monochromatic beam energy is selected by rotating the doublecrystal assembly. The 2nd crystal has an additional rotational freedom driven either by a

https://doi.org/10.1017/S0885715613000900 Published online by Cambridge University Press

stepper motor or by a piezo actuator, the latter offering finer tuning. Both crystals also have rotational adjustment (so called roll axes) along the beam which allows the exit beam to be steered horizontally. Part of DCM commissioning was to optimize the roll axes in order to have the beam fixed horizontally when changing the energy. Finally, it has to be noted that the maximum operating energy of the beamline, 50 keV, is imposed by the limited length of the 2nd crystal. Just after the monochromator we have a non-cooled 4 blade slit system (supplied by JJ X-rays).

Beam diagnostics are of particular importance during commissioning and operation. The MSPD beamline is particularly well equipped with diagnostic tools. Two direct beam visualization devices are positioned approx. 1 m before and after the DCM. These devices consist of a CVD diamond (in the white/pink beam) or YAG (in the monochromatic beam) crystal placed in the beam at an angle of 45º (Fuchs *et al.*, 2007). The CVD/YAG material is highly fluorescent and the footprint of the beam on the crystal is recorded online using a standard CCD camera positioned at 90º relative to the beam. The screens being in UHV environment, the CCD camera views the screen through an optical viewport. With this method, the shape, dimensions and position of the beam can be easily surveyed by using an appropriate frame grabber and software. CVD/YAG screens can be remotely moved out of the beam path, the one before the DCM is water cooled.

Intensity monitoring of the monochromatic beam is achieved by X-ray beam position monitors (XBPM) (Alkire *et al.*, 2000) positioned just after the DCM and before each of the MSPD experimental stations. These devices consist of four PIN diodes directed towards an Fe foil and positioned ~20 mm behind the foil at cardinal points (top/bottom/left/right). When passing through the foil, backscattering fluorescence is detected by the four diodes and with appropriate weighting of each signal, the exact position of the beam on the foil can in principal be extracted. On MSPD, we restrict ourselves to adding up the signal of all the diodes, hence we use the XBPM as a global intensity monitor. Since the signals from the diodes are very low currents, highly sensitive current reading electrometers are necessary. Such electrometer allowing to measure currents in the 100 pA to 1 mA range have been designed and installed at ALBA (Lidon-Simon *et al.*, 2012). Moreover, the XBPM at ALBA offers the possibility to remotely position three foils of different thickness (0.5, 2 and 5 μm) which allows tuning of the strength of the output signal intensity depending on the monochromatic beam energy. Of course, there is the possibility to have these foils out of the beam path.

https://doi.org/10.1017/S0885715613000900 Published online by Cambridge University Press

All optical components are under UHV environment, the low pressure is achieved and monitored using standard ion pumps and pressure gauges. The final barrier between the beamline UHV and ambient pressure is located 28 m from the source, already in the experimental hutch, and consists of two beryllium windows, one position for each of the mirror/non-mirror operation modes, glued on a standard CF flange.

The High Pressure diffraction station

The first experimental station is positioned 31 m from the source and is dedicated to High Pressure/Microdiffraction techniques. The requirement is hence to obtain the smallest beam size at the sample position. This is achieved on MSPD by using Kirkpatrick Baez (KB) focusing geometry which consists of two independent elliptically bent reflecting surfaces. On MSPD, the reflecting surfaces are graded $[W/Si]_{100}$ multilayers with average layer spacing d_v=3 nm and d_h=2.6 nm for vertical and horizontal focusing. The first harmonic of the multilayer reflection is used. Mirrors are positioned 1.1 m and 0.7 m before the sample position for vertical and horizontal focusing, respectively. Mirror dimensions, bending parameters and multilayer choice have been appropriately selected to operate in the 20 to 50 keV energy range. Indeed, higher energies, hence higher penetration depth, are preferred for angular dispersive HP stations since the monochromatic beam is expected to pass through relatively massive diamond anvils cells. With this device we obtained a minimum beam size of 14 x 10 μm^2 at the HP sample position. The downstream PD station is also designed (horizontal and vertical translation of the whole diffractometer) to accept the beam as focused by the same KB equipment.

The HP "diffractometer" is essentially two towers of stacked rotation/tilt/translation stages supplied by Huber Diffraktionstechnik. The sample is mounted on a tower consisting, from bottom to top, of an XYZ stage/ a rotation stage/an XY stage (here Y refers to the direction along the beam and Z vertical). This configuration allows alignment of a very small sample (< 50 μm) on the sample stage rotation axis, and then the rotation axis and sample into the beam. The alignment of the sample on the rotation axis is essential as data are generally collected while rotating the sample over a typical 5-30^o range, in order to increase powder averaging. Before the sample, a collimator and pin-hole aperture ranging from 50 to 200 μm in diameter serve as anti-scatter slits in order to clean the beam from parasitic scattering. The detector of the HP station is a Rayonix SX165 with 2048 x 2048 pixels of 80 x 80 μm^2 dimension. The detector is on a tower

https://doi.org/10.1017/S0885715613000900 Published online by Cambridge University Press

consisting of a stack of XYZ translation, a rotation and a tilt stage. The min/max achievable sample-detector distances are 100 mm and 500 mm respectively. Early in 2013, the HP station will be equipped with a remote control pressure calibration setup, an online visualization of the sample and a remote pressure drive system. The HP station has already been open to friendly and official user experiments starting in June 2012.

In order to demonstrate the potential of the HP station, we present here preliminary results collected on a rare-earth orthovanadate, $NdVO_4$ compound. The interest in this system is due to its wide range of potential applications: cathodoluminescent, thermophosphors, scintillators and as a nuclear-waste storage candidate (Panchal *et al*. 2011). Powder X-ray diffraction patterns of $NdVO_4$ under high pressure were acquired by the angle dispersive method using an Almax-Boehler diamond anvil cell (DAC) (Boehler, 2006). The sample was loaded into a 300 μm hole of an indented inconel X750 gasket inside a DAC with 700 μm culet size. A ruby sphere was loaded with the sample to determine the pressure by the fluorescence method (Mao *et al.*, 1986). A 16:3:1 methanol-ethanol-water mixture was used as pressure transmitting medium (Klotz, *et al.*, 2009). The wavelength of the monochromatic X-ray beam was 0.4246 Å which corresponds to the Sn *K*-edge. The X-ray beam was focused to 14×10 μm^2 using the KB mirrors. The diffraction patterns were collected with a 400 mm sample to detector distance up to 12 GPa pressure. The 2D Debye-Scherrer circles were registered as 2D raw frames, and processed into 1D powder patterns using FIT 2D software (Hammersley *et al.*, 1996). A typical two 2D image of $NdVO_4$ diffraction collected at 1 GPa is shown in Fig. 2a. The Rietveld refinement, performed using the program GSAS (Larson and von Dreele, 1994) confirmed the tetragonal zircon-type structure ($I4_1/amd$) at ambient conditions (Fig 2b).When applying pressure, it was reported that these compounds undergo a structural phase transition to a much denser phase, either scheelite or in some cases to monazite phase. Results obtained on MSPD confirmed the latter case, the zircon-to-monazite phase transition. A more detailed discussion of the XRD data will be presented elsewhere.

https://doi.org/10.1017/S0885715613000900 Published online by Cambridge University Press

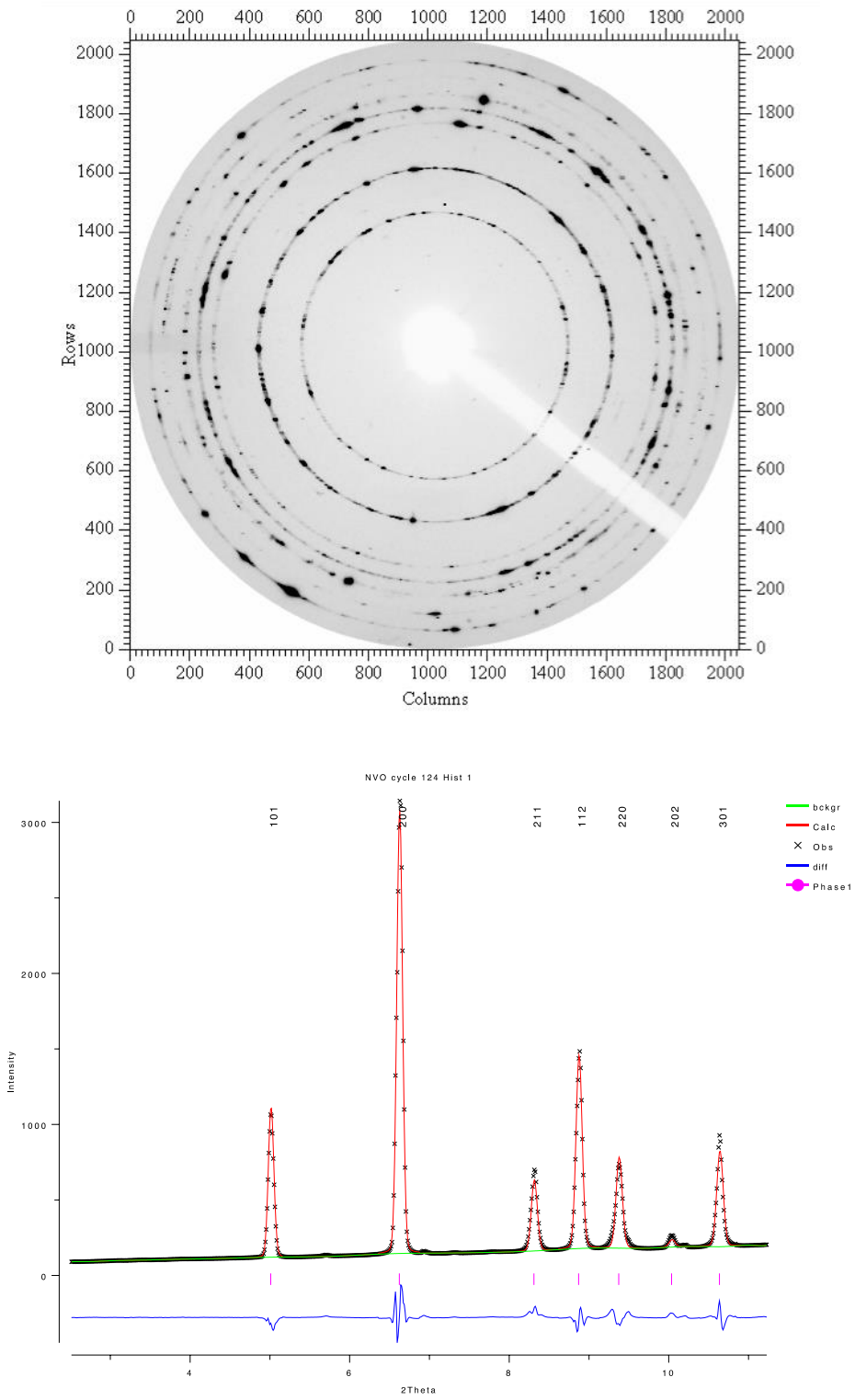

Figure 2: a) Raw 2D image of $NdVO_4$ at P=1 GPa, b) the corresponding image processed into a 1D pattern with observed, calculated and difference XRD profiles.

https://doi.org/10.1017/S0885715613000900 Published online by Cambridge University Press

The High resolution/High throughput Powder Diffraction station

Downstream of the HP station, located at 35 m from the source, stands the Powder Diffraction station. It essentially consists of a heavy duty 3 concentric circle diffractometer which was delivered by Huber Diffractionstechnik. The inner circle supports a Eulerian cradle for the sample which can be optionally removed. The middle circle supports the high throughput position sensitive detector, so called MYHTEN detector (Bergamaschi, 2010) allowing simultaneous acquisition of powder patterns over a 40º 2θ range at ms time resolution. On the outer circle is mounted a 13-channel analyzer/YAP scintillator/PMT tube detector system allowing data collection at high angular resolution. Either 111 or 220 silicon Bragg reflections can be selected for the analyzers (Peral *et al.*, 2011). At the time of the proceeding, November 2012, the Powder Station just started operation and the high resolution setup was not yet commissioned.

In order to evaluate the performance of the powder station, we present a powder diffraction experiment measured on a Riboflavin compound. The sample was loaded into a 0.5 mm diameter capillary. Powder diffraction patterns were collected at 0.8847 Å wavelength, over 3^{o}-49.1^{o} 2θ range and 14 minutes acquisition time with the Mythen-II detector (Bergamaschi *et al.*, 2010) at room and low temperature. Integrated intensities were extracted from the RT pattern with DAJUST (Vallcorba *et al.*, 2012) (Chi=10.6, Rwp=0.248), and processed with cluster-based direct methods (Rius, 2011) as implemented in the XLENS_p6 program [www.icmab.es/crystallography/software] to solve the riboflavin structure ($C_{17}H_{20}N_4O_6$, Z=4. Space group=$P2_12_12_1$, a=20.2121, b=15.2157 and c=5.3708 Å) (see figure 3).

https://doi.org/10.1017/S0885715613000900 Published online by Cambridge University Press

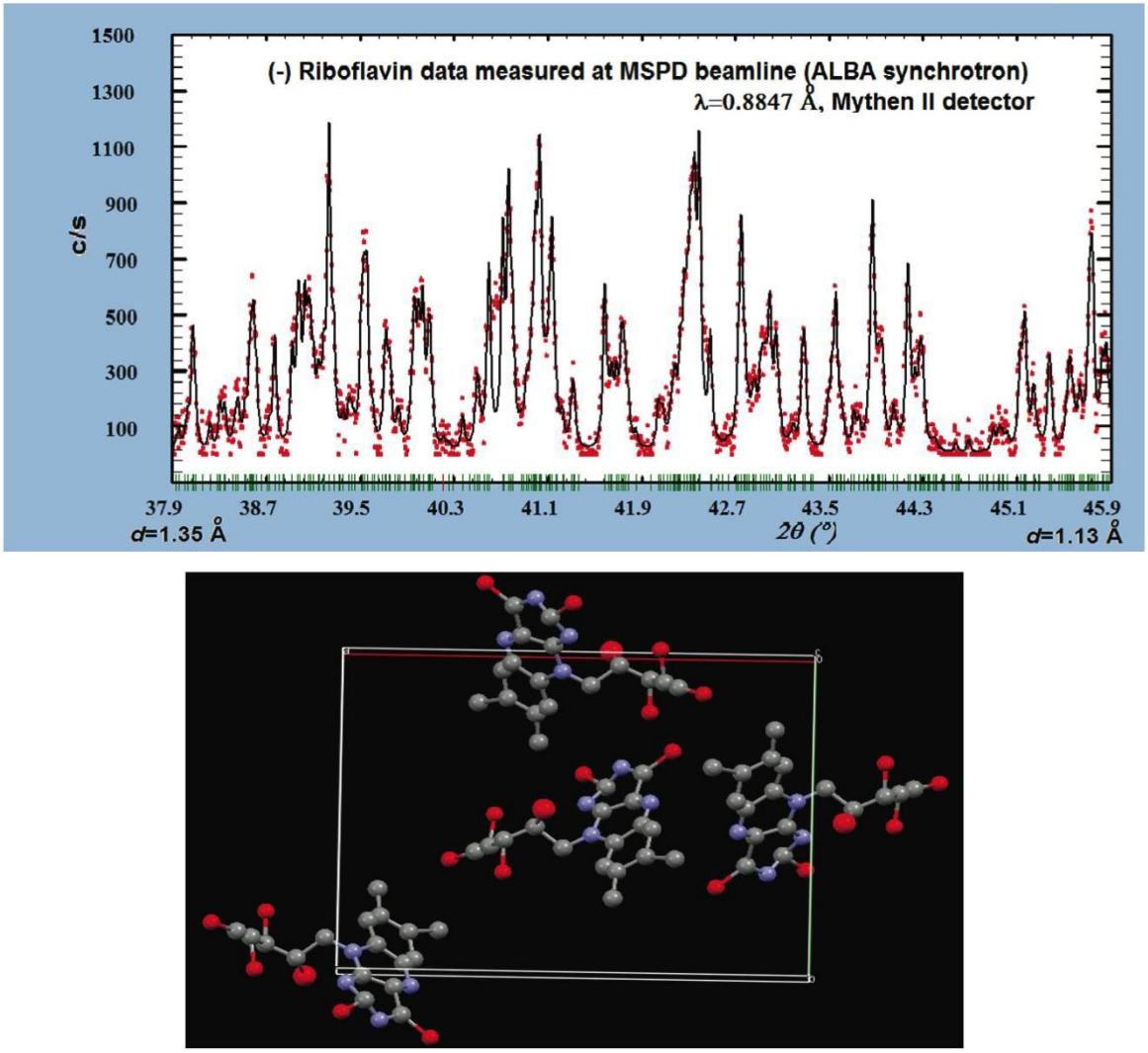

Figure 3: Observed and calculated powder diffraction patterns of riboflavin (only the high-resolution portions are shown); experimental details can be found in the text. A perspective view of unit cell of riboflavin is reproduced.

Summary

In this paper, we have described the installation and preliminary commissioning of the Material Science Powder Diffraction Beamline of the recent ALBA synchrotron facility. We have essentially focused on the optics since commissioning started in November 2011 already. The HP station has already been routinely used in 2012 and the first users' papers are already submitted. The Powder station has just started operation but demonstrates promising capabilities.

https://doi.org/10.1017/S0885715613000900 Published online by Cambridge University Press

Acknowledgments

I. Peral thanks the Spanish Ministerio de Ciencia e Innovación Tecnológica (project MAT2009-07967). The authors thank D. Errandonea for support in the High Pressure data collection and J. Rius, O. Vallcorba and C. Frontera for support in the MYTHEN data collection.

Alkire, R. W., Rosenbaum, G. and Evans, G. (**2000**). Design of a vacuum-compatible high-precision monochromatic beam-position monitor for use with synchrotron radiation from 5 to 25 keV," J. Synchrotron Radiat. **7**, 61-68.

Bergamaschi, A., Cervellino, A., Dinapoli, R., Gozzo, F., Henrich, B., Johnson, I., Kraft, P., Mozzanica, A., Schmitt, B. and Shi, X. (**2010**). "The MYTHEN detector for X-ray powder diffraction experiments at the Swiss Light Source," J. Synchrotron Radiat. **17**, 653–668.

Boehler, R. (**2006**). "New diamond cell for single-crystal x-ray diffraction," Rev. Sci. Instrum. **77**. 115103.

Fuchs, M. R., Holldack, K., Reichardt, G. and Mueller, U. (**2007**). "Transmissive Imaging X-Ray Beam Position Monitors (XBPM) for Protein Crystallography (PX) Beamlines," AIP Conf. Proc. **879**, 1006-1009. [doi: 10.1063/1.2436232].

Hammersley, A. P., Svensson, S. O., Hanfland, M., Fitch, A. M. and Haussermann, D. (**1996**). "Two-dimensional detector software: From real detector to idealised image or two-theta scan," High Pressure Res. **14**, 235-248.

Klotz, S., Chervin, J.-C., Munsch, P. and Le Marchand (**2009**). "Hydrostatic limits of 11 pressure transmitting media," J. Phys. D: Appl. Phys. **42**, 075413.

Larson, A. C. and von Dreele, R. B. (**1994**). *GSAS: General Structure Analysis System* (Report LAUR 86-748). Los Alamos, New Mexico: Los Alamos National Laboratory.

Lidon-Simon, J., Fernandez-Carreiras, D., Gigante, J., Jamroz, J., Klora, J. and Matilla, O. (**2011**). "Low current meausrements at ALBA," WEPMS025: Proceedings of ICALEPCS2011, Grenoble, France Hardware, 1032-1035.

Mao, H. K., Xu, J. and Bell, P. M. (**1986**). "Calibration of the ruby pressure gauge to 800 kbar under quasi-hydrostatic conditions," J. Geophys. Res., [Solid Earth Planets] **91**, 4673-4676.

Panchal, V., Errandonea, D., Segura, A., Rodriguez-Hernandez, P., Munoz, A., Lopez-Moreno, S. and M. Betonelli, (**2011**). "The electronic structure of zircon-type orthovanadates: Effects of high-pressure and cation substitution," J. Appl. Phys. **110**, 043723 and the references therein.

Peral, I., McKinley, J., Knapp, M. and Ferrer, S, (**2011**). "Design and construction of multicrystal analyser detectors using Rowland circles: application to MAD26 at ALBA," J. Synchrotron Radiat. **18**, 842-850.

Rius, J. (**2011**). "Direct phasing from Patterson syntheses by δ recycling," Acta Crystallogr., Sect. A: Found. Crystallogr., A68, 77-81.

Vallcorba, O., Rius, J., Frontera, C., Peral, I. and Miravitlles, C. (**2012**). "*DAJUST*: a suite of computer programs for pattern matching, space-group determination and intensity extraction from powder diffraction data*," J. Appl. Crystallogr.* **45**, 844-848

https://doi.org/10.1017/S0885715613000900 Published online by Cambridge University Press